Design and Implementation of Predictive Current Controller for Photovoltaic Grid-Tie Inverter

MAHMOUD SALEM[1,2] and YOUSRY ATIA[1]
1- Electronics Research Institute ,El-Tahrir St., Dokki, Giza, EGYPT
2-Taif University, Faculty of Engineering, Electrical Eng. Dept, KSA
Masalem32@yahoo.com, yousry_atia@yahoo.com

Abstract: - This paper presents simplified predictive current controller for 3-ph PWM voltage source inverter connected to the utility grid via filter inductance. By controlling inductance voltage drop, the inverter voltage and hence the injected current can be controlled. The proposed predictive control technique operates with constant switching frequency using space-vector modulation (SVM). In each switching period, the proposed control algorithm computes the required inverter average voltage vector in α–β reference frame in order to follow up the reference current at the end of the switching period. The proposed technique has no need for coordinate transformations or PI controllers. The proposed controller is verified by simulation using MATLAB/Simulink, and is experimentally verified using a fixed point microcontroller (Maple microcontroller). Detailed implementation of the proposed hardware is presented. Both simulations and experimental results are presented in the paper.

Key-Words: - Predictive Current Control, SVM, Grid-Tie, Distributed Power Generation Systems.

1 Introduction

As a new means of power generation, distributed generation (DG) systems are experiencing rapid growth along with the increasing demand for electrical energy [1]. Most DG systems need power electronic converters, often referred as inverters, to realize power conversion, grid interconnection and control optimization [2]. Pulse- width-modulated (PWM) voltage source inverters (VSI) are widely applied in DG systems. Due to quick response and accurate control, the current controlled PWM voltage source inverters are usually preferred for high performance and continuous ac power supplies that needed to produce a sinusoidal ac output [3]. The main task of the current-controlled PWM voltage source inverters is to force the current vector in the three phase load according to a reference trajectory. The performance of the converter system largely depends on the applied current control technique [4]. When current control is used, the inverter output currents are measured and compared with reference signals, the errors being used as an input to the PWM modulator, which provides the inverter switching signals.

Mainly, there are three types of current controllers used in voltage source inverters; ramp comparator current controller, hysteresis current controller, and predictive current controller. The ramp comparator controller compares the error current signal to a carrier waveform to generate the inverter firing pulses [5]. Predictive current controllers calculate the voltage of the inverter which forcing the load current vector to follow the reference current trajectory. In a hysteresis current controller, the hysteresis comparators are used to impose a dead band or hysteresis around the reference current [6].

Current control strategies based on space vector PWM (SVPWM) are widely employed [7]. A SVPWM-based current controller separates current error compensation and PWM functions, making it possible to exploit the advantages of SVPWM as well as to independently design the overall control structure [8]. SVPWM has many advantages such as constant switching frequency, well defined output harmonic spectrum, optimum switching patterns, and excellent dc-link voltage utilization [9].

The objective of this paper is to present a simplified direct current control scheme for three-phase PWM inverter based on a predictive approach. The proposed predictive control technique operates with constant switching frequency using space-vector

modulation. For this purpose, a predictive control algorithm was developed to compute the required inverter average voltage vector, to be generated during each switching period Ts, in order to cancel out the line current errors at the end of the switching period. The computed inverter average voltage vector, in α–β reference frame, is converted into a sequence of switching states (adjacent voltage vectors) by means of SVM technique. Finally, the developed predictive control algorithm was tested both in simulations and experimentally, using fixed-point microcontroller.

2 Grid-Connected Inverter Modeling

Fig.1 shows schematic diagram of the proposed current controlled grid-connected system. The system is composed of distributed power generation unit, three phase two-levels inverter connected to the utility grid via filter inductance Ls. The active and reactive power is delivered to the grid and controlled by current controller. The converter in this case works as inverter where the power is delivered to the grid. The dc source simulates the distributed photovoltaic or wind energy system.

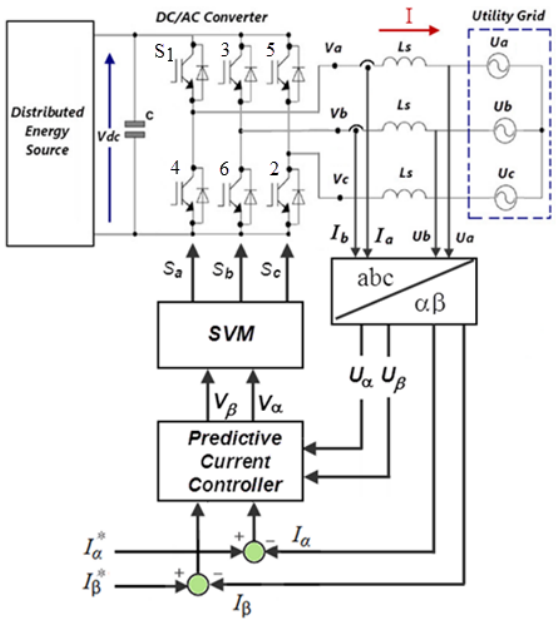

Fig.1 Current controlled grid-tie DC/AC converter.

The proposed predictive current control scheme is based on the computation of the inverter average voltage vector in α–β reference frame v_α, v_β using a predictive current control algorithm, which makes instantaneous line currents equal to their reference values at the end of each sampling period. For this reason, current errors in α-β reference frame and grid voltage vector u_α, u_β are used as input data variables for predictive current control block as shown in Fig. 1. At the beginning of each switching period T_s, the inverter average voltage vector $v_{\alpha\beta}$, which allows cancellation of current tracking errors at the end of the switching period, is computed. Then, SVM technique is used to generate a sequence of inverter switching states, to achieve the control objective with constant switching frequency.

2.1 Inverter modeling in α-β reference frame

Considering the grid supply is an ideal voltage source, and neglecting inductance resistance R, Fig. 2 shows the simplified equivalent circuit for ac side of the inverter in the α-β reference frame.

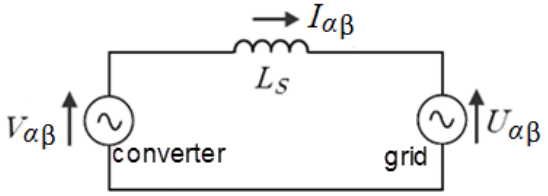

Fig.2 Equivalent circuit of grid-tie inverter in α-β reference frame.

From Fig. 2, the relation between the inverter output voltage (v) and the grid voltage (u) in α-β frame can be given by:

$$\begin{bmatrix} v_\alpha(t) \\ v_\beta(t) \end{bmatrix} = \begin{bmatrix} u_\alpha(t) \\ u_\beta(t) \end{bmatrix} + L_S \frac{d}{dt} \begin{bmatrix} i_\alpha(t) \\ i_\beta(t) \end{bmatrix} \quad (1)$$

From (1), the inverter voltage and hence the injected current can be controlled by controlling the voltage drop on the input choke coils.

Using a discrete approximation of Eq. (1), the inverter vector can be expressed as:

$$\begin{bmatrix} v_\alpha(k) \\ v_\beta(k) \end{bmatrix} = \begin{bmatrix} u_\alpha(k) \\ u_\beta(k) \end{bmatrix} + \frac{L_S}{T_s} \begin{bmatrix} \Delta i_\alpha(k) \\ \Delta i_\beta(k) \end{bmatrix} \quad (2)$$

Where:

$$\Delta i_{\alpha\beta}(k) = i_{\alpha\beta}(k+1) - i_{\alpha\beta}(k) \ . \quad (3)$$

Since the control objective is to force line currents $i_{\alpha\beta}$ to be equal to their reference values $i^*_{\alpha\beta}$ at the next sampling instant (k+1), the following equation can be used:

$$\Delta i_{\alpha\beta}(k) = i^*_{\alpha\beta}(k+1) - i_{\alpha\beta}(k) \quad (4)$$

The reference currents in α-β frame $i^*_{\alpha\beta}$ can be set directly as a two orthogonal sinusoidal signals synchronized with $u_{\alpha\beta}$ for unity power factor operation as follows:

$$i^*_{\alpha\beta} = Au_{\alpha\beta} \quad (5)$$

Where *A* is a constant gain.

The proposed predicted reference current is assumed to be as follows:

$$i^*_{\alpha\beta}(k+1) = Au_{\alpha\beta}(k) + \left(Au_{\alpha\beta}(k) - Au_{\alpha\beta}(k-1)\right) \quad (6)$$

Substituting (4), (5) and (6) in (2), the inverter output voltage vector can be calculated as follows:

$$\begin{bmatrix} v_\alpha(k) \\ v_\beta(k) \end{bmatrix} = \begin{bmatrix} u_\alpha(k) \\ u_\beta(k) \end{bmatrix} + \frac{L_S}{T_s} \begin{bmatrix} 2Au_\alpha(k) - Au_\alpha(k-1) - i_\alpha(k) \\ 2Au_\beta(k) - Au_\beta(k-1) - i_\beta(k) \end{bmatrix} \quad (7)$$

Using space vector modulation (SVM), Eq. 7 can be used to generate PWM signals for VSI.

3 Space Vector PWM

SVPWM have good utilization of the DC link voltage, low current ripple and relative easy hardware implementation. Compared to the sinusoidal PWM, the SVPWM have 15% higher utilization ratio of the voltage [10]. These features make it suitable for high voltage high power applications, such as renewable power generation. A three-phase two-level inverter provides eight possible switching states, made up of six active and two zero switching states as shown in Fig.3. Active vectors divide plane for six sectors. Any reference vector V_s is represented in α-β-plane as:

$$V_s = V_\alpha + jV_\beta = |V_s|\cos(\theta) + j|V_s|\sin(\theta) \quad (8)$$

The amplitude and phase of the reference voltage vector can be calculated from v_α, v_β as follows:

$$V_s = \sqrt{\left(v_\alpha^2 + v_\beta^2\right)}$$
$$\theta = \tan^{-1}\left(\frac{v_\beta}{v_\alpha}\right) \quad (9)$$

Since VSI cannot instantaneously generate V_s, the space-vector PWM principle consists in producing T_s -periodic voltage whose average value equals V_s, by generating V_n during t_1 and V_{n+1} during t_2 for sector number (n). Since $t_1 + t_2 \le T_s$, these voltages must be completed over the switching period T_s by V_0 and/or V_7. Several solutions are possible [11], and the one which minimizes the total harmonic distortion consists in applying V_0 and V_7 during the same duration. Vector V_s can be realized with two active and one zero vector. For first sector ($0 < \theta \le \pi/3$), as shown in Fig. 4, V_s can be generated by V_1, V_2, and V_0 that applied in times t_1, t_2, and t_0 respectively.

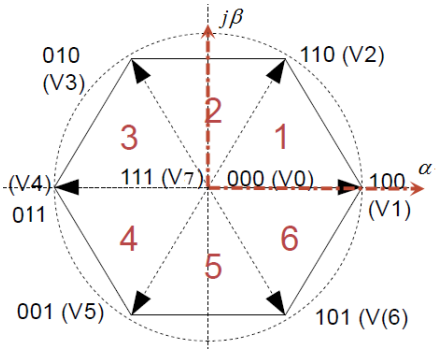

Fig. 3 Vectors and sectors of SVM plane.

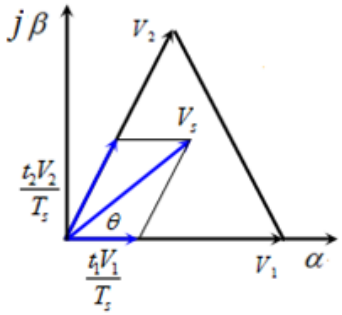

Fig. 4 Voltage vector in sector 1.

From Fig. 4 in sector 1:

$$V_s = \left(\frac{t_1 V_1}{T_s} + \frac{t_2 V_2}{T_s}\cos(\pi/3)\right) + j\frac{t_2 V_2}{T_s}\sin(\pi/3) \quad (10)$$

Where: $|V_1| = |V_2| = 2V_{dc}/3$, $V_0 = 0$

$$V_\alpha = \frac{2t_1}{3T_s}V_{dc} + \frac{2t_2}{3T_s}V_{dc}\cos(\pi/3) \quad (11)$$

$$V_\beta = \frac{2t_2}{3T_s}V_{dc}\sin(\pi/3) \quad (12)$$

Equating components of (8) with (11) and (12), t_1 and t_2 can be found in sector 1 as:

$$t_1 = \frac{\sqrt{3}V_s T_s}{V_{dc}}\sin\left(\frac{\pi}{3} - \theta\right) \quad (13)$$

$$t_2 = \frac{\sqrt{3}V_s T_s}{V_{dc}} \sin(\theta) \quad (14)$$

Repeating the previous step in each sector leads to several expressions of t_1 and t_2.

General expressions for these times can be written in a unified way as [12]:

$$t_1 = \frac{\sqrt{3}V_s T_s}{V_{dc}} \sin(\frac{\pi}{3} - \theta_1) \quad (15)$$

$$t_2 = \frac{\sqrt{3}V_s T_s}{V_{dc}} \sin\theta_1 \quad (16)$$

$$t_0 = T_s - t_1 - t_2 \quad (17)$$

Where: $\theta_1 = \theta - (n-1)*\frac{\pi}{3}$, $0 < \theta_1 \le \pi/3$ (18)

4 Simulation Results

The proposed system is simulated on MATLAB/Simulink environment. The system is composed from three-phase VSI, DG DC source, filter inductor, utility grid, and the proposed controller. The simulated system parameters values that used in simulation are given in Table I.

TABLE I
THE SIMULATED SYSTEM PARAMETERS

Vdc	113 V
Urms	36 V
Ls	18 mH
Ts	100 µs
fs	10 kHz

The inputs of the controller function are the dc source voltage, sampling time Ts, two phase voltages and two phase currents where the output is the PWM signals for six transistors and other monitoring signals.

The results are taken both in steady state and in transient conditions. Fig. 5 shows the three phase currents in steady state operation. Fig. 6 shows the phase-A voltage and current. It is shown that the current is in phase with the voltage for unity power factor operation.

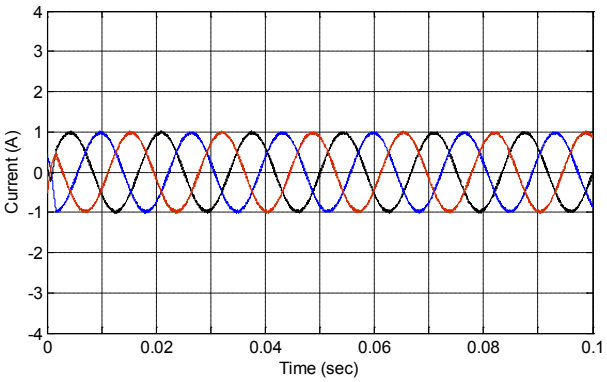

Fig. 5 Three phase currents in steady state.

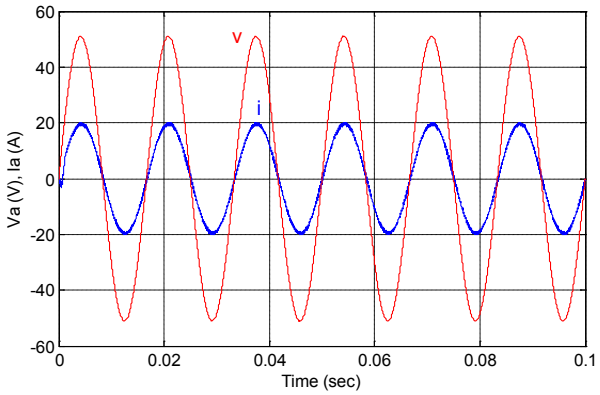

Fig. 6 Phase-A voltage and current in steady state, Scale; V: 20V/div, I: 1A/div.

Fig. 7 shows the relation between inverter output line voltage and grid line voltage. It shows that the inverter output voltage is advanced on the grid voltage for inverter mode of operation.

Fig. 8 shows transient response and step change in reference current. The three phase line currents are step up at 0.05 sec., where Fig. 9 shows phase-A voltage and current during step change in reference current.

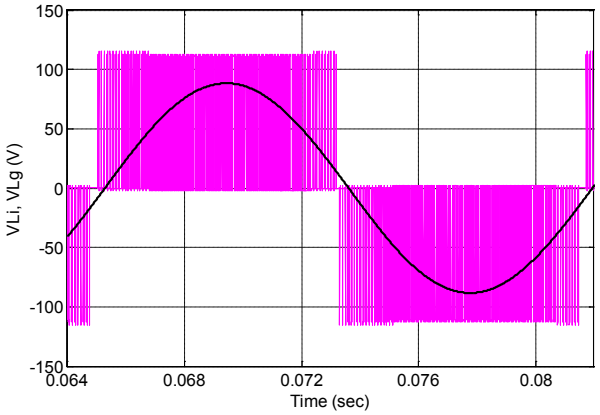

Fig. 7 Inverter and grid line voltages.

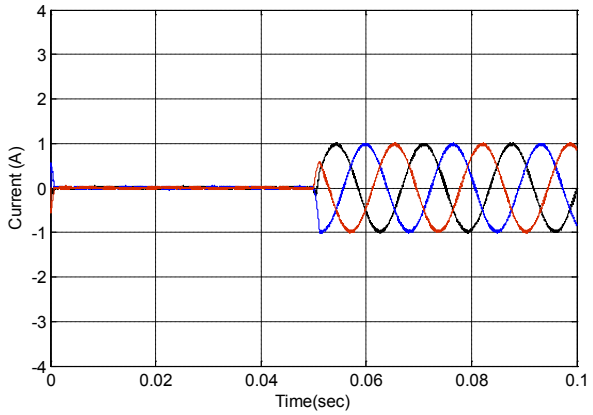

Fig. 8 3-phase current during step change in reference current.

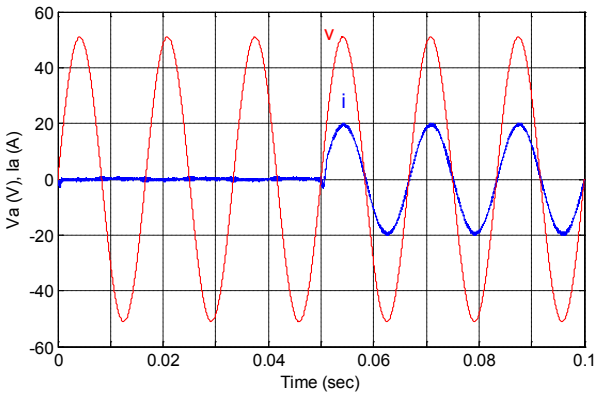

Fig. 9 Phase-A voltage and current during step change in reference current, Scale; V: 20V/div, I: 1A/div.

5 Experimental System

In order to verify the performance of the theoretically studied grid-connected system, experimental test circuit was built. The circuit is composed of 3-phase VSI, 4-channel isolation amplifier; inductor filter, 3-phase y-connected transformer, and circuit breaker connected to three phase utility grid. The grid–connected inverter prototype was controlled by Maple microcontroller board equipped with fast processor speed, fast sampling ADC and high speed 16-bit timer/ counter.

In experimental work, a three-phase transformer was used to decrease the three-phase source voltage from 380 to 62V. The dc source was connected to the inverter's dc link. Fig. 10 shows the experimental setup circuit. Digital storage oscilloscope (DSO-2090 USB) with PC-interface is used to monitor and plot the experimental results.

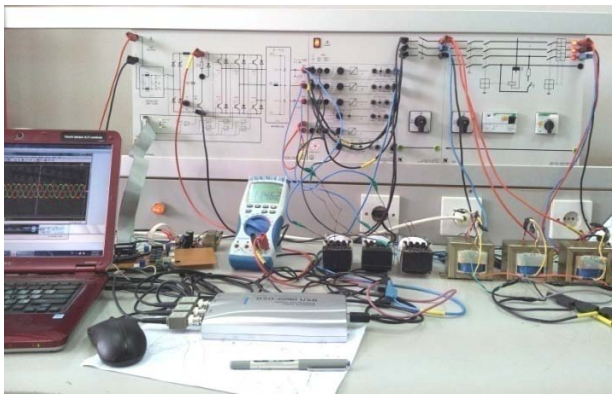

Fig. 10 Experimental setup circuit.

5.1 Maple-based microcontroller board

The core of Maple microcontroller (MC) board as shown in Fig. 11 is STM32F103RB ARM Cortex M3 processor with lots of peripherals. This providing increased computational power desired by more advanced users. The processor is 32-bit fixed-point microcontroller with the main features as listed in Table II.

Fig.11 Maple microcontroller board.

As the ADC of the MC is uni-polar, signal conditioning circuit is built to prepare the voltage and current signals to fits the ADC polarity and voltage. Also interfacing circuit is built to connect the MC board to VSI. The interfacing circuit accepts two phase voltage and two phase current signals from the system and outputs six gating signals and protection signal to the inverter. Fig. 12 shows the MC and signal conditioning circuit board.

5.2 Voltage Angle Determination Algorithm

An efficient algorithm is built to determine the voltage angle θ without using long time consuming (atan2) trigonometric function. An arc cosine lookup

table is used to determine the angle of V_β then simple comparison instructions for V_α is carried out to determine θ as shown in algorithm flowchart in Fig.13.

Table II
MICRCOCONTROLLER BOARD SPECIFICATIONS

Board	Maple
Device	STM32F103RB
Clock	72 MHz
SRAM	20 Kbytes
Flash	128 Kbytes
A/D	18 channel, 12-bit resolution
Conversion Time	1μs
Timers	Four 16-bit timer/counter with 4 separate 4 compare registers.
Digital I/O	39
Analog I/O	16
Communication	USB

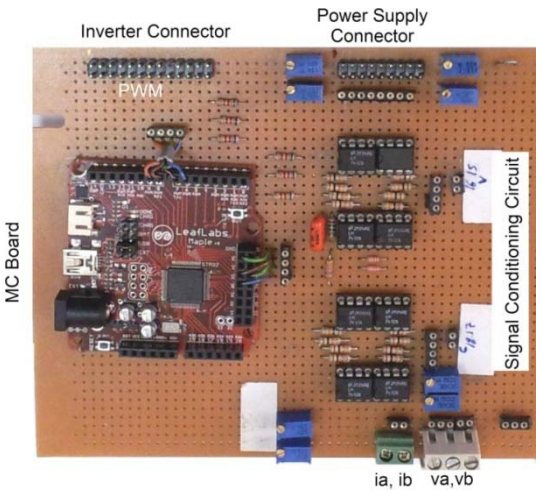

Fig.12 Microcontroller and signal conditioning board

5.3 Implementation of SVPWM

Maple microcontroller contains two advanced-control timers consist of a 16-bit auto-reload counter driven by programmable prescaler [13]. It can be used for a variety of purposes, including generating output PWM waveforms with complementary PWM with dead-time insertion. Each timer contains 4 separate channels that can be programmed in to generate the switching wave-forms computed from the SVM algorithm. Timer 1 is used to generate interrupt each 100 μsec for 10 kHz switching frequency of SVM. Three compare registers are used to compare the computed values for generating three PWM signals and their complement separated by a dead time. The counter will count up from zero to a value corresponding to one half of the switching period (as shown in Fig. 14), and then counts down to zero, then generate interrupt request, and counts up again. So, the interrupt service subroutine can be programmed for constant intervals. In this subroutine, PWM for six switches of VSI are computed and generated. The PWM width that must be generated for upper VSI switches (S1, S3, and S5) at different sectors are given in Table III. The complementary of those pulses are generated for lower VSI switches with programmed dead time. The dead time is set to 3μs between upper and lower switch at the same leg of the inverter.

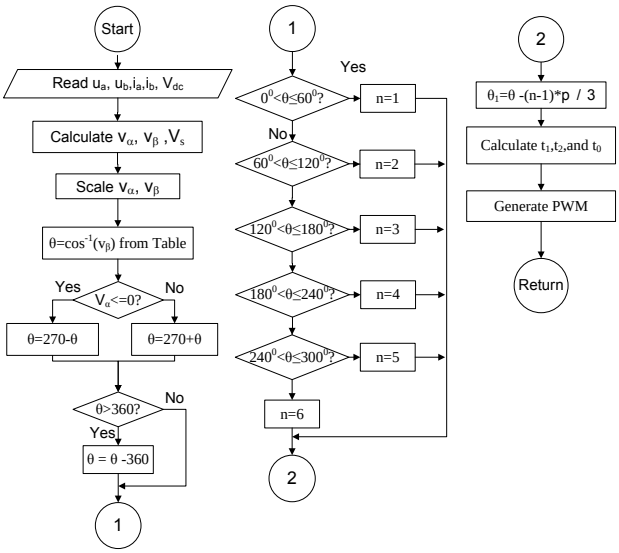

Fig.13 Flowchart for voltage angle determination and PWM generation routine.

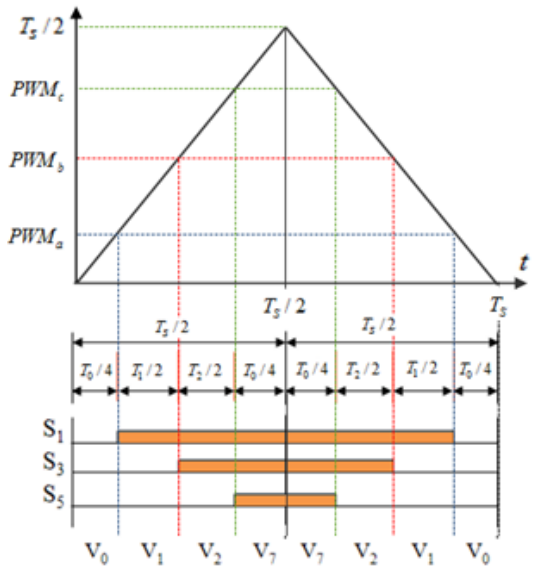

Fig. 14 Inverter switches waveforms and corresponding compare register values in sector 1.

TABLE III.
PULSE WIDTH vs SECTORS.

n	S1	S3	S5
1	$t_1+t_2+t_0/2$	$t_2+t_0/2$	$t_0/2$
2	$t_1+t_0/2$	$t_1+t_2+t_0/2$	$t_0/2$
3	$t_0/2$	$t_1+t_2+t_0/2$	$t_2+t_0/2$
4	$t_0/2$	$t_1+t_0/2$	$t_1+t_2+t_0/2$
5	$t_2+t_0/2$	$t_0/2$	$t_1+t_2+t_0/2$
6	$t_1+t_2+t_0/2$	$t_0/2$	$t_1+t_0/2$

6 Experimental Results

Experimental verifications of the theoretical results are explained in this section. Fig. 15 shows phase-A voltage and phase-A current where they are in-phase for unity power factor operation, whereas Fig. 16 shows the three phase current injected to the grid.

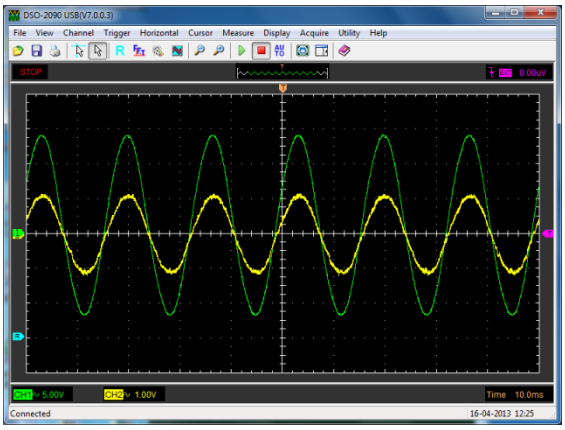

Fig. 15 Experimental phase current and voltage of the system. Scale: 1A/div, 20V/div, and10ms/div.

A step change in reference current from 0A to1A is carried out in Fig 17 and Fig. 18. Fig. 17 shows phase-A voltage and phase-A current during this step change, and Fig. 18 shows three-phase current during step change.

Fig. 19 shows PWM signals for switch 1 and switch 3 and the difference between them, which represents inverter line voltage.

Fig. 20 shows switch-1 PWM signal with phase-A current. As the inverter switches signals are active low PWM, so that as the PWM pulses becomes narrower, as the phase current increases. In this figure the constant switching frequency is clear as 10 kHz, where the sample time is 100μs.

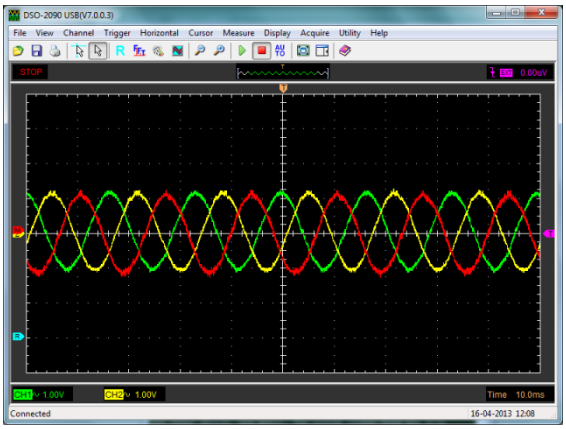

Fig. 16 Experimental three phase current fed to the grid. Scale: 1A/div, 10ms/div.

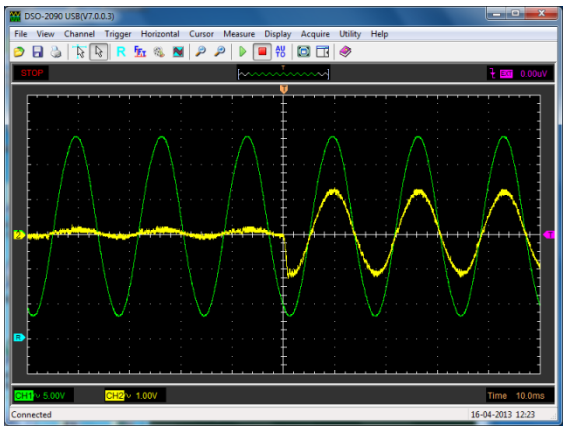

Fig. 17 Experimental step change in phase-A current with the phase-A voltage. Scale: 20V/div, 1A/div, 10ms/div.

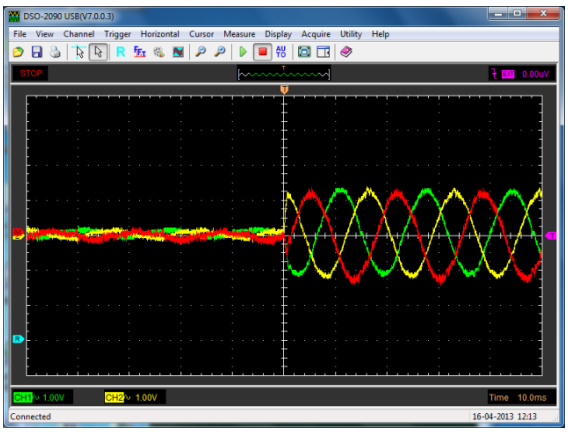

Fig. 18 Experimental step change in reference current. Scale: 1A/div, 10ms/div.

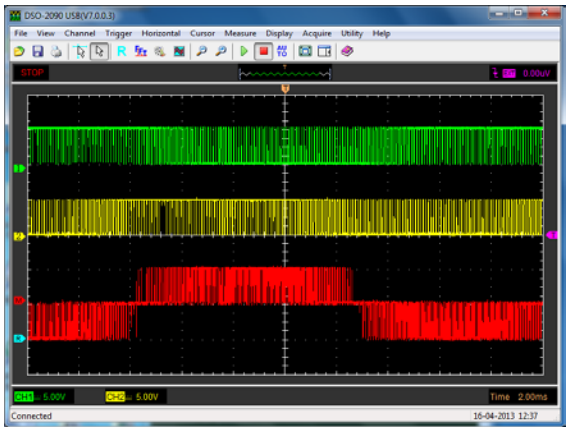

Fig. 19 Experimental PWM signals for the system Scale: 5V/div, 200ms/div.

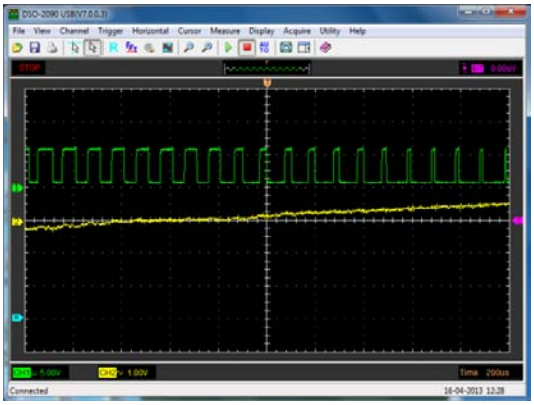

Fig. 20 Experimental PWM signal for T1 and phase-A current. Scale: 5V/div, 1A/div, and 200μs/div.

7 Conclusion

This paper proposed simplified controller for controlling grid connected distributed power generating system. The proposed system is simulated theoretically by MATLAB/Simulink and verified experimentally by a fixed point microcontroller. Both simulation and experimental work are coincide and gave excellent results in both steady state and transient operation. Instead of complex and expensive digital signal processor, this work introduced a simple and cheap fixed point microcontroller to execute all computations and control functions of the proposed technique.

References:

[1] Qingrong Zeng and Liuchen Chang, An Advanced SVPWM-Based Predictive Current Controller for Three-Phase Inverters in Distributed Generation Systems, *IEEE Transaction on Industrial Electronics*, Vol. 55, NO. 3, March 2008.

[2] F. Blaabjerg, etal, Overview of control and grid synchronization for distributed power generation systems, *IEEE Transaction on Industrial Electronics*, vol. 53, no. 5, pp. 1398–1409, Oct. 2006.

[3] M. Prodanovic and T. C. Green, Control and filter design of three-phase inverters for high power quality grid connection, *IEEE Transactions on Power Electronics*, vol. 18, pp. 373-380, Jan. 2003.

[4] M. P. Kazmierkowski and L. Malesani, Current control techniques for three-phase Voltage-Source PWM Converters: A survey, *IEEE Transaction on Industrial Electronics* , Vol. 45, pp. 691-703, Oct. 1998.

[5] E. Twining and D. G. Holmes, Grid current regulation of a three-phase voltage source inverter with an LCL input filter, *IEEE Transactions on Power Electronics*, vol. 18, pp.888-895, May 2003.

[6] Qingrong Zeng; Liuchen Chang; Study of Advanced Current Control Strategies for Three-Phase Grid-Connected PWM Inverters for Distributed Generation , *Proc. of IEEE Conf. on Control Application*, Pp.1311– 316, Aug,2005.

[7] D. G. Holmes, D. A. Martin, Implementation of a direct digital predictive current controller for single and three phase voltage source inverters, *IEEE 31 Annual Meeting of Ind. App. Conf.* 1996.

[8] Bouafia, J. Gaubert, and F. Krim. Design and implementation of predictive current control of three-phase PWM rectifier using space-vector modulation (SVM), *Energy Conversion and Management* 51 (2010) 2473–2481.

[9] Bouafia, J. Gaubert, and F. Krim, Predictive Direct Power Control of Three-Phase Pulse width Modulation (PWM) Rectifier Using Space-Vector Modulation (SVM), *IEEE Transactions on Power Electronics*, Vol. 25, No. 1, Jan. 2010

[10] D. Rathnakumar et al., A New Software Implementation of Space Vector PWM, *Department of Electrical Eng., Government college of Technology*, India, 2005.

[11] Y.Y. Tzou, H.J. Hsu, FPGA realization of space-vector PWM control IC for three-phase PWM inverters, *IEEE Transactions on Power Electronics*, Vol. 12, No 6, pp 953-963, 1997.

[12] Atmel AVR495, AC Induction Motor Control Using the Constant V/f Principle and a Space-vector PWM Algorithm, *Application Note*.
[13] Reference Manual RM0008 (PDF); definitive resource for peripherals on the STM32F1 line, http://www.st.com.